Cooling Rate of Chondrule Estimated from Compositionally-Zoned Olivine

Hitoshi Miura[1] and Tetsuo Yamamoto[2]

[1]Nagoya City Univeristy, Japan, [2]Kobe University, Japan
email: miurah@nsc.nagoya-cu.ac.jp

1. Compositional zoning of olivine

Olivine phenocrysts in chondrules exhibit remarkable compositional zonings, which record the crystallization environments in the early solar nebula.

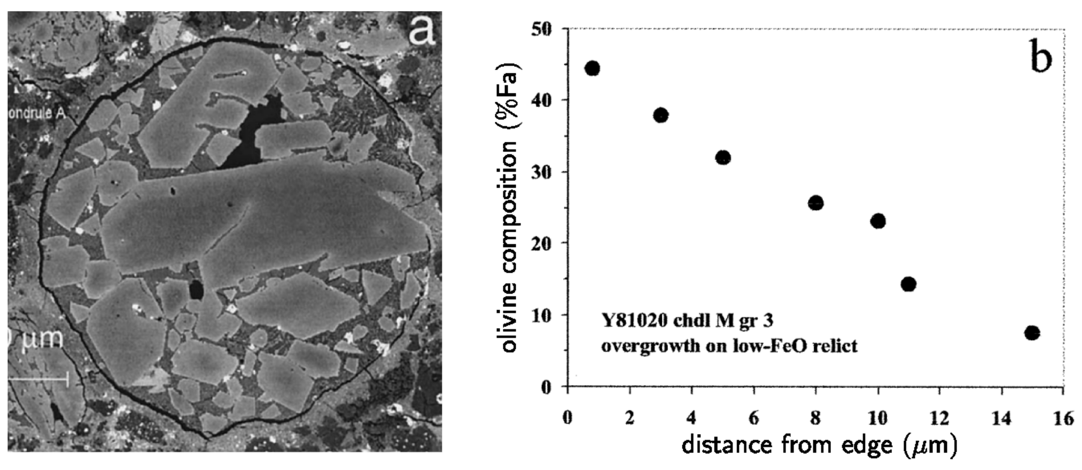

Figure 1: (a) BSE image of type II porphyritic chondrule. (b) Compositional zoning profile. [4]

> Question
> What is the origin of linear zoning?
> How can we infer the cooling rate from the zoning profile?

2. Fractional crystallization

The key process of the chondrule-melt crystallization is elemental partitioning between growing phenocrysts and the remaining liquid. Solidification under rapid cooling condition causes compositional gradient in the liquid. The compositional gradient leads to significant modifications in the compositional zoning profile in minerals.

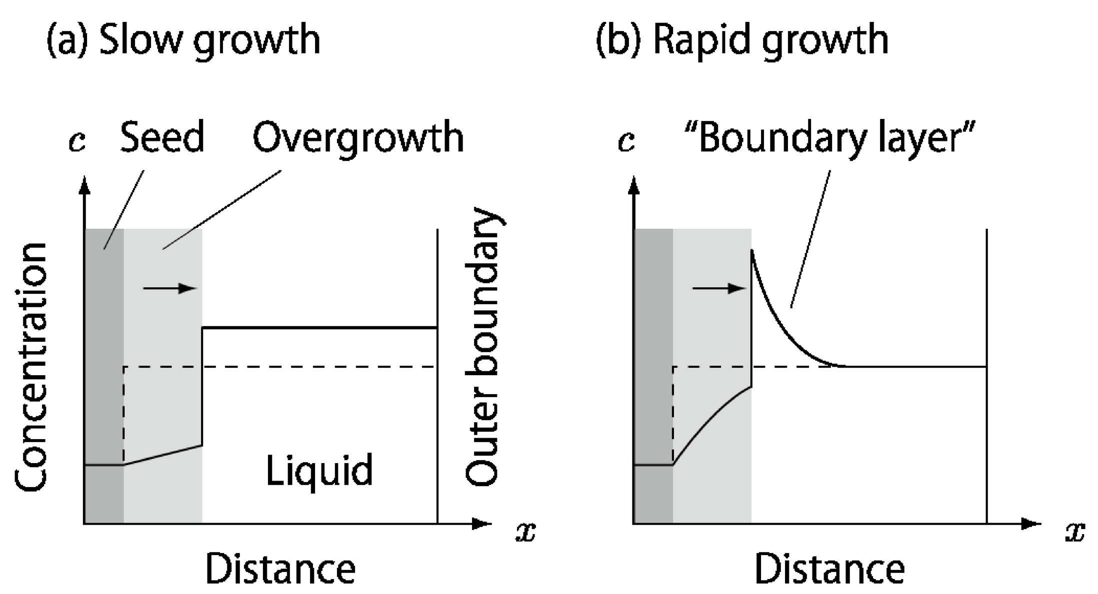

Figure 2: Models of fractional crystallizations.

> Motivation
> To decipher the records of the solar system history preserved in the chondrule textures, we should obtain comprehensive understanding of the dynamics of solidification!!

> Purpose of this study
> We elucidate the formation process of the linear zoning profile of relict olivines in chondrules.

3. Basic equations

Crystal growth associated with solute diffusion in a liquid has been formulated as a moving boundary problem [3]:

$$\frac{\partial c_{\rm L}}{\partial t} = \frac{\partial}{\partial x'}\left(D_{\rm L}\frac{\partial c_{\rm L}}{\partial x'}\right) + V\frac{\partial c_{\rm L}}{\partial x'} \qquad (x'>0), \tag{1}$$

where $c_{\rm L}$ is the concentration of FeO in liquid; x', coordinate co-moving with the solid-liquid interface; $D_{\rm L}$, diffusivity in liquid; V, growth velocity. The interface is fixed at $x'=0$. Eq. (1) must be solved with the initial condition given by

$$c_{\rm L}(x';0) = c_{\rm L0} = c_{\rm L}^{\rm e}(T_0), \tag{2}$$

the boundary conditions given by

$$c_{\rm L}(\infty;t) = c_{\rm L0} = c_{\rm L}^{\rm e}(T_0) \tag{3}$$

and

$$\frac{\partial c_{\rm L}}{\partial x} + \frac{V}{D_{\rm L}}[c_{\rm L}^{\rm e}(T) - c_{\rm S}^{\rm e}(T)] = 0 \quad \text{at } x'=0, \tag{4}$$

where $c_{\rm L0}$ is the initial concentration in the liquid; $c_{\rm L}^{\rm e}$ and $c_{\rm S}^{\rm e}$, the equilibrium concentrations in liquid and solid, respectively; T_0, initial temperature at which the solid co-exists with liquid in equilibrium. $c_{\rm L}^{\rm e}$ and $c_{\rm S}^{\rm e}$ are given by an ideal solution model [1].
We decrease temperature T at a constant rate $R_{\rm c}$ to trigger the crystal growth.

4. Numerical results

As the temperature decreases, the solid-liquid interface moves rightward. Figure 3 shows that $c_{\rm L}$ rises ahead of the moving interface as a result of the partitioning. Note that a concentration $c_{\rm S}$ in the solid increases monotonically with x. The area in which the composition changes steeply is called an initial transient [3]. $c_{\rm S}$ exceeds $c_{\rm L0}$ at $x = 16.5\ \mu{\rm m}$, which gives a width of the initial transient $d_{\rm f}$.

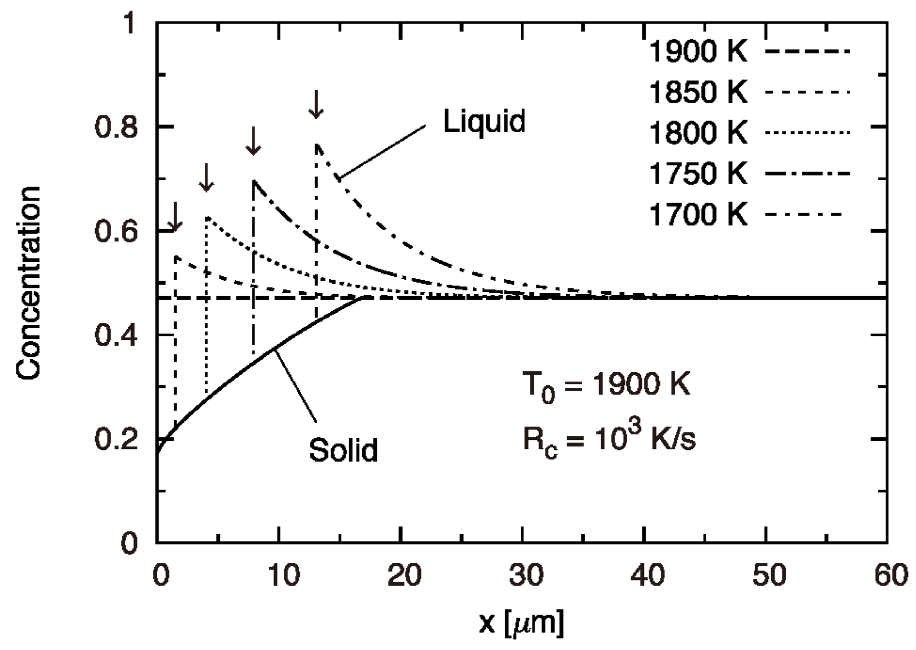

Figure 3: Numerical result for $T_0 = 1900$ K and $R_{\rm c} = 10^3$ K s^{-1}.

The position of interface $d(t)$ is well fitted (see Fig. 4) by

$$d(t) = V_0 t_0 (e^{t/t_0} - 1), \tag{5}$$

where V_0 is initial growth velocity and t_0 is time constant. This indicates that V increases exponentially with time:

$$V(t) = V_0\, e^{t/t_0}. \tag{6}$$

In this case, the best-fit values are $V_0 = 26.2\ \mu{\rm m\ s^{-1}}$ and $t_0 = 0.124$ s, respectively.

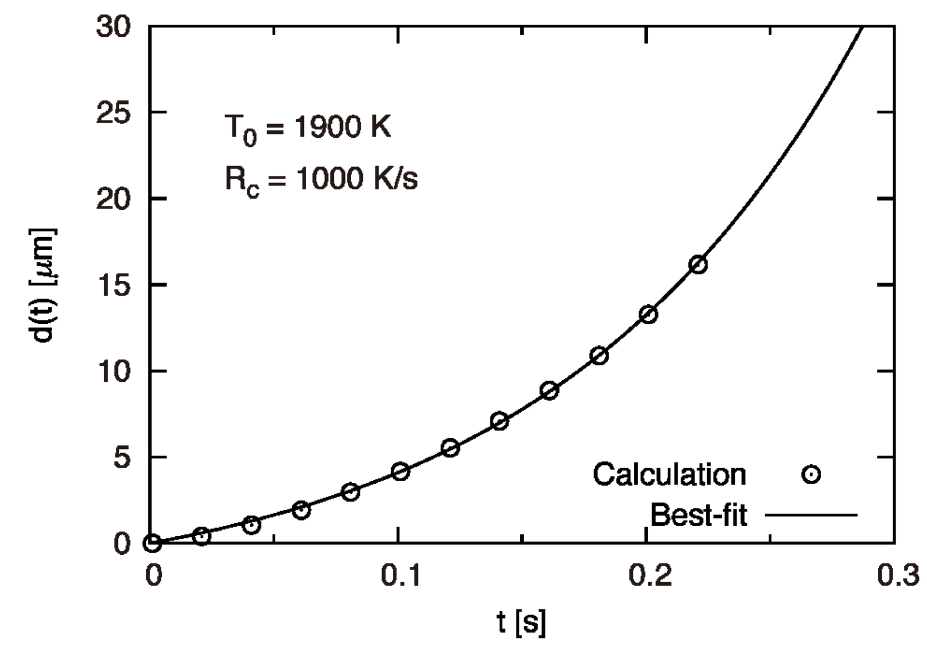

Figure 4: Interface position $d(t)$ as a function of time (open circles). The solid curve shows the best-fit using Eq. (5).

Figure 5 shows the dependence of the width of the initial transient $d_{\rm f}$ (panel a) and the time constant t_0 (panel b) on $R_{\rm c}$. Note that these parameters show a power-law dependence on $R_{\rm c}$: $d_{\rm f} \propto R_{\rm c}^{-1/2}$ and $t_0 \propto R_{\rm c}^{-1}$.

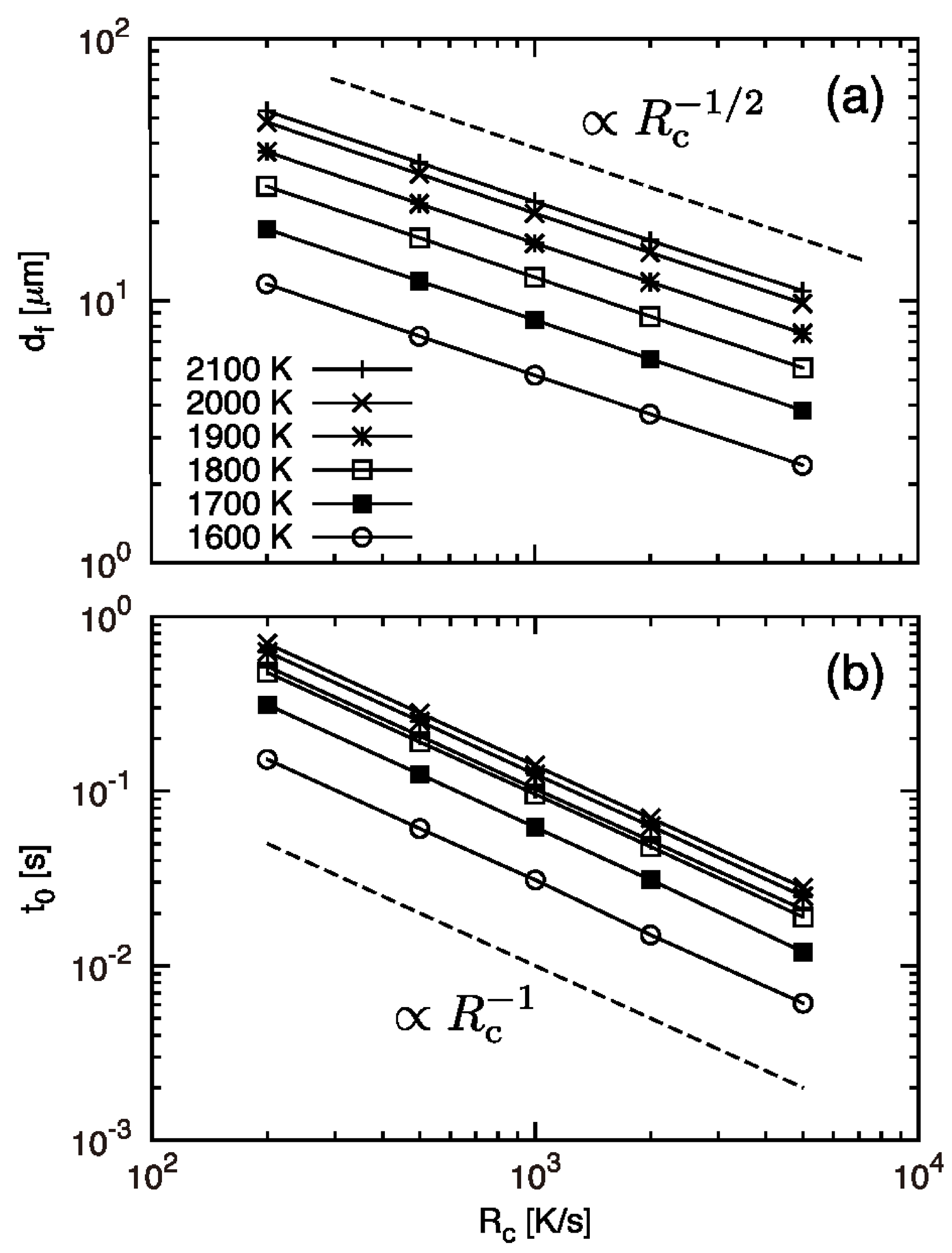

Figure 5: Dependence of the initial transient parameters on the cooling rate $R_{\rm c}$.

5. Analysis of compositional zoning

We found an empirical relation (see Miura & Yamamoto, in prep. for the physical grounds):

$$t_0 \approx \frac{1}{2} t_{\rm sol} = \frac{1}{2}\frac{\Delta T_c}{R_{\rm c}}, \tag{7}$$

where $t_{\rm sol} \equiv \Delta T_c / R_{\rm c}$ is solidification time and ΔT_c is the temperature difference between the liquidus and solidus for a given concentration. Taking Eq. (6) into account, the solute distribution in the crystal in the initial transient is expressed (see Miura & Yamamoto, in prep. for derivation) by

$$c_{\rm S}(x) \approx k_0 c_{\rm L0}\left[1 + (1-k_0)\sqrt{\frac{2\pi R_{\rm c}}{D_{\rm L}\Delta T_c}}\cdot x\right], \tag{8}$$

where $k_0 \equiv c_{\rm S}^{\rm e}/c_{\rm L}^{\rm e}$. Note that $c_{\rm S}$ increases linearly with x.
From $c_{\rm S}(d_{\rm f}) = c_{\rm L0}$, we immediately obtain

$$d_{\rm f} \approx \frac{1}{k_0}\sqrt{\frac{D_{\rm L}\Delta T_c}{2\pi R_{\rm c}}}. \tag{9}$$

Figure 6 shows that these analytic formulas well reproduce the numerical results for wide ranges of T_0 and $R_{\rm c}$.

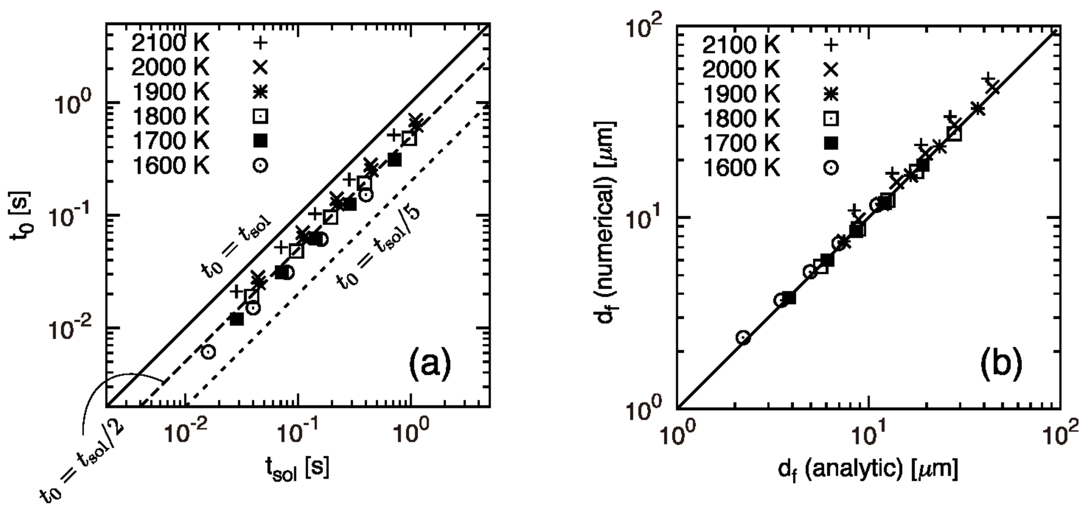

Figure 6: Comparison between the analytic formulae and the numerical results.

6. Discussion

From Eq. (8), we obtain

$$R_{\rm c} \approx \frac{D_{\rm L}\Delta T_c}{2\pi k_0^2 (1-k_0)^2 c_{\rm L0}^2}\left(\frac{dc_{\rm S}}{dx}\right)^2 \sim 200 - 2000\ {\rm K\ s^{-1}} \tag{10}$$

for $D_{\rm L} = 10^{-6}$–$10^{-5}\ {\rm cm^2\ s^{-1}}$, $\Delta T_c = 200$ K, $k_0 = 0.4$, $c_{\rm L0} = 0.5$, and $dc_{\rm S}/dx = 300\ {\rm cm^{-1}}$. These estimates are orders of magnitude higher than the cooling rate of $0.01 - 1\ {\rm K\ s^{-1}}$ inferred from furnace-based experiments.
Aerodynamic drag heating induced by nebula shocks is one of the plausible mechanisms to melt chondrule precursor silicate grains. However, it does not satisfy simultaneously following two thermal constraints [2] such as rapid heating ($\sim 10^4 - 10^6\ {\rm K\ hr^{-1}}$ sufficient to prevent isotopic fractionation of sulfur in primary troilite and consecutive slower cooling ($\lesssim 10^3\ {\rm K\ hr^{-1}}$) inferred by the furnace-based experiments. Much more rapid cooling suggested by our theory supports shock waves produced in the solar nebula, which can cause the rapid heating and consecutive rapid cooling as the chondrule-forming events. These shocks include planetesimal bow shock, nebula shocks in less-dusty environments , and shock waves induced by X-ray flares.

> Conclusion
> The most important outcome of this study is to propose analytic relations between the compositional zoning profile and the growth conditions of crystals. The relations enable one to reveal the growth conditions, in particular, the cooling rate at the formation of chondrules. The cooling rate is one of the most important but undetermined key parameters in astromineralogy and in clarifying thermal history in the solar nebula. Our approach may provide a new diagnostic method for compositional zonings in minerals.

References

[1] N. L. Bowen and J. F. Schairer. The system, MgO-FeO-SiO$_2$. *American Journal of Science*, 29:151–217, 1935.

[2] Hitoshi Miura and Taishi Nakamoto. Shock-wave heating model for chondrule formation: Prevention of isotopic fractionation. *Astrophys. J.*, 651:1272–1295, 2006.

[3] V. G. Smith, W. A. Tiller, and J. W. Rutter. A mathematical analysis of solute redistribution during solidification. *Canadian Journal of Physics*, 33:723–745, 1955.

[4] John T. Wasson and Alan E. Rubin. Ubiquitous low-feo relict grains in type ii chondrules and limited overgrowths on phenocrysts following the final melting event. *Geochim. Cosmochim. Acta*, 67:2239–2250, 2003.